Inorganic Chemistry

Article

Reactions of Trivacant Wells–Dawson Heteropolytungstates. Ionic Strength and Jahn–Teller Effects on Formation in Multi-Iron Complexes

Travis M. Anderson, Xuan Zhang, Kenneth I. Hardcastle, and Craig L. Hill*

Department of Chemistry, Emory University, Atlanta, Georgia 30322

Reaction of α-$P_2W_{15}O_{56}^{12-}$ and Fe(III) in a saturated NaCl solution produces a trisubstituted Wells–Dawson structure with three low-valent metals, α-$(Fe^{III}Cl)_2(Fe^{III}OH_2)P_2W_{15}O_{59}^{11-}$ (**1**). Dissolution of this species into 1 M NaBr (Br$^-$ is noncoordinating) gives the triaquated species α-$(Fe^{III}OH_2)_3P_2W_{15}O_{59}^{9-}$ (**2**). Ionic strength values of 1 M or greater are necessary to avoid decomposition of **1** or **2** to the conventional sandwich-type complex, $\alpha\beta\beta\alpha$-$(Fe^{III}OH_2)_2$-$Fe^{III}_2(P_2W_{15}O_{56})_2^{12-}$ (**3**). If the pH is greater than 5, a new triferric sandwich, $\alpha\alpha\beta\alpha$-$(NaOH_2)(Fe^{III}OH_2)Fe^{III}_2$-$(P_2W_{15}O_{56})_2^{14-}$ (**4**), forms rather than **3**. Like the previously reported Wells–Dawson-derived sandwich-type structures with three metals in the central unit ($[TM^{II}Fe^{III}_2(P_2W_{15}O_{56})(P_2TM^{II}_2W_{13}O_{52})]$,$^{16-}$ TM = Cu, Co), this complex has a central α-junction and a central β-junction. Thermal studies suggest that **4** is more stable than **3** over a wide range of temperatures and pH values. The intrinsic Jahn–Teller distortion of d-electron-containing metal ions incorporated into the external sites of the central multimetal unit impacts the stoichiometry of their incorporation (with a consequent change in the inter-POM-unit connectivity, where POM = polyoxometalate). Reaction of nondistorting Ni(II) with the diferric lacunary sandwich-type POM $\alpha\alpha\alpha\alpha$-$(NaOH_2)_2Fe^{III}_2(P_2W_{15}O_{56})_2^{16-}$ (**5**) produces $\alpha\beta\beta\alpha$-$(Ni^{II}OH_2)_2Fe^{III}_2$-$(P_2W_{15}O_{56})_2^{14-}$ (**6**), a Wells–Dawson sandwich-type structure with two Ni(II) and two Fe(III) in the central unit. All structures are characterized by ^{31}P NMR, IR, UV–vis, magnetic susceptibility, and X-ray crystallography. Complexes **4** and **6** are highly selective and effective catalysts for the H_2O_2-based epoxidation of alkenes.

Introduction

Polyoxometalates (POMs) containing Keggin and Wells–Dawson moieties are of fundamental and practical interest.[1-4] The ability to extensively alter the molecular properties (potentials, charges, sizes, etc.) of POMs, coupled with their chemically robust nature, has led to a wide range of applications. A number of processes (in particular oxidation and acid-dependent reactions) are catalyzed by POMs, and this work continues to be the subject of considerable ongoing research.[5-10] The development of POMs as catalysts derives

in part from the fact they are often invoked as structural models for reactive metal oxide surfaces.[11] In this context, trivacant lacunary heteropolytungstates are of particular interest because they present the opportunity to modify the surface properties of metal-oxide-like structural units via the replacement of several adjacent high-valent tungsten centers with low-valent metals (Co(II) and Fe(III), for example).[12]
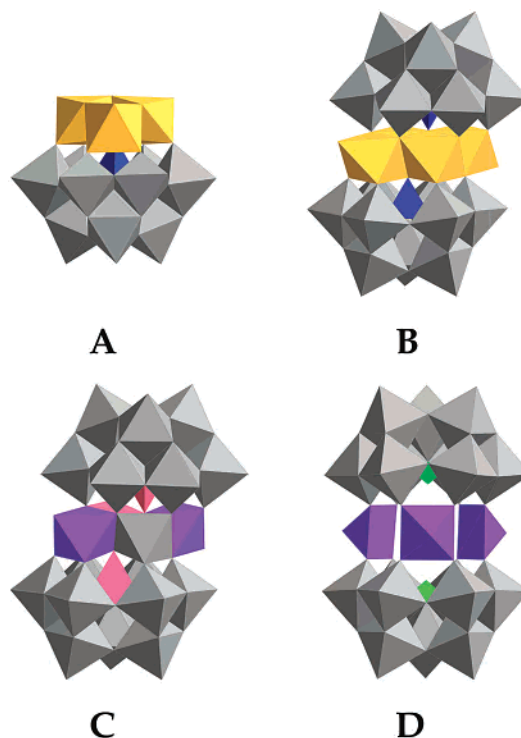
The reactions of d-electron transition metal cations with trivacant POM species are very complex. First, the three

---

* To whom correspondence should be addressed. E-mail: chill@emory.edu.
(1) Pope, M. T. *Heteropoly and Isopoly Oxometalates*; Springer-Verlag: Berlin, 1983.
(2) *Polyoxometalates: From Platonic Solids to Anti-retroviral Activity*; Pope, M. T., Müller, A., Eds.; Kluwer Academic Publishers: Dordrecht, Netherlands, 1993.
(3) Topical issue on polyoxometalates: Hill, C. L., Guest Ed. *Chem. Rev.* **1998**, *98*, 1–389.
(4) *Polyoxometalate Chemistry: From Topology via Self-Assembly to Applications*; Pope, M. T., Müller, A., Eds.; Kluwer Academic Publishers: Dordrecht, Netherlands, 2001.
(5) Hill, C. L.; Prosser-McCartha, C. M. *Coord. Chem. Rev.* **1995**, *143*, 407–455.
(6) Okuhara, T.; Mizuno, N.; Misono, M. *Adv. Catal.* **1996**, *41*, 113–252.

(7) Mizuno, N.; Misono, M. *Chem. Rev.* **1998**, *98*, 199–218.
(8) Kozhevnikov, I. V. *Chem. Rev.* **1998**, *98*, 171–198.
(9) Neumann, R. *Prog. Inorg. Chem.* **1998**, *47*, 317–370.
(10) Katsoulis, D. E. *Chem. Rev.* **1998**, *98*, 359–388.
(11) The M_3O_{13} unit, a common feature in POMs, is structurally analogous to close packed units on steps and corners of catalytically active metal oxide surfaces. (a) Reference 1. (b) Day, V. W.; Klemperer, W. G. *Science* **1985**, *228*, 533–541. (c) Finke, R. G.; Rapko, B.; Saxton, R. J.; Domaille, P. J. *J. Am. Chem. Soc.* **1986**, *108*, 2947–2960. (d) Reference 2. (e) Rapko, B. M.; Pohl, M.; Finke, R. G. *Inorg. Chem.* **1994**, *33*, 3625–3634. (f) Pohl, M.; Lin, Y.; Weakley, T. J. R.; Nomiya, K.; Kaneko, M.; Weiner, H.; Finke, R. G. *Inorg. Chem.* **1995**, *34*, 767–777. (g) Reference 3.
(12) (a) Katsoulis, D. E.; Pope, M. T. *J. Am. Chem. Soc.* **1984**, *106*, 2737–2738. (b) Liu, J. G.; Ortega, F.; Sethuraman, P.; Katsoulis, D. E.; Costello, C. E.; Pope, M. T. *J. Chem. Soc., Dalton Trans.* **1992**, 1901–1906.

---

substituted metal octahedra can be corner-sharing (A-type) or edge-sharing (B-type).[13] Previous reports have established that the A-type is more common with a number of A-α- or A-β-X(MOH$_2$)$_3$W$_9$O$_{37}$$^{n-}$ (where M = d-electron transition metal center and X = central heteroatom) structures reported.[12,14-20] Second, A-type trivacant POMs can react with d-electron metals to form either the trisubstituted parent ("monomeric") structure or sandwich-type structures resulting from the fusion of two A-α-XW$_9$O$_{34}$$^{n-}$ units via three corner-sharing transition metal cations (formula (MOH$_2$)$_3$(α-PW$_9$O$_{34}$)$_2$$^{n-}$, where M = any 3d metal).[21-23] In addition, B-type trivacant POMs, such as α-P$_2$W$_{15}$O$_{56}$$^{12-}$ or B-PW$_9$O$_{34}$$^{9-}$, can lead to at least two product structures (Figure 1). One involves filling of the trivacant site by three edge-sharing transition metal MO$_6$ units (to regenerate the parent Wells−Dawson or Keggin structures, respectively), and the other involves fusion of two trivacant POMs units (via a rhombus of four edge-sharing transition metal ions) to form a sandwich-type structure.[24-47]
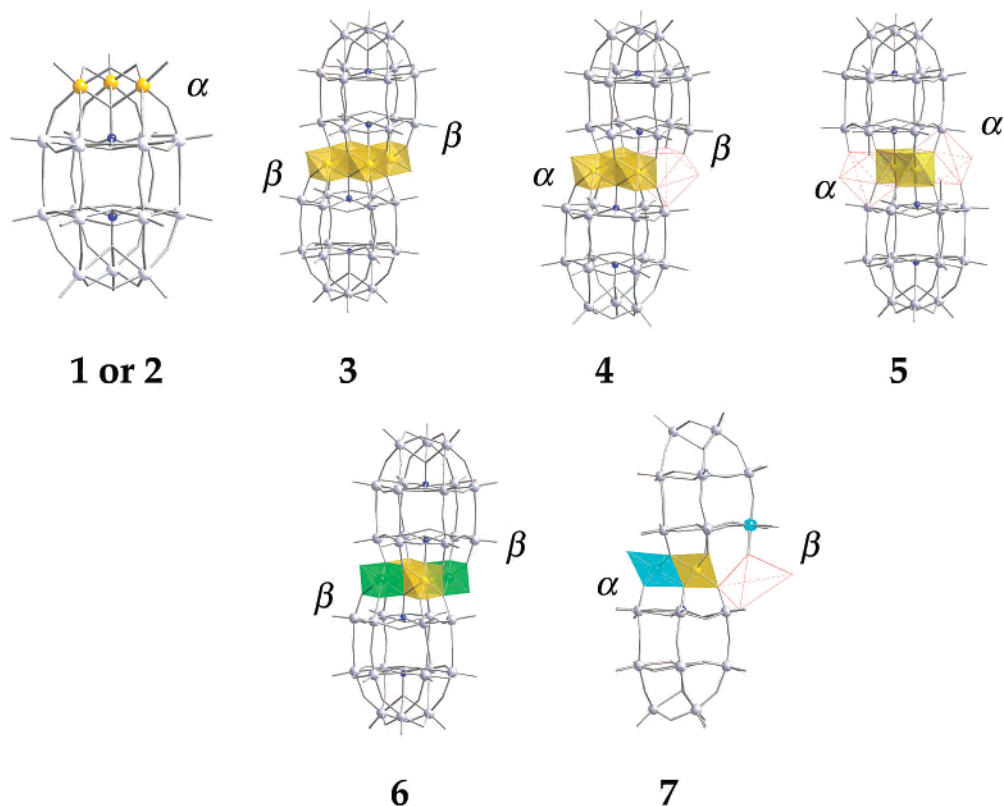

Figure 1. Polyhedral representations of species derived from trivacant B-type lacunary Keggin structures. (A) Trisubstituted parent Keggin structure. (B) Conventional sandwich-type structure. (C) Neumann derivative of Zn-Tourné complex. (D) M$_3$ sandwich-type structure.

There are many previous reports investigating the role of transition metal cations on the consequent POM structure.[12,14-51] For B-type trivacant POMs, most of these reports have reached the same conclusion. High-valent metals such as V(V) give the trisubstituted parent species while low-valent metals such as Cu(II), Co(II), and Zn(II) give the dimeric sandwich-type species.[32,52] Finke and co-workers

(13) There are two possible non-Baker−Figgis isomers in trivacant Keggin structures. The A-type species is formed by removal of one corner-sharing MO$_6$ octahedron from each of three bridging M$_3$O$_{13}$ triads. The B-type species is formed by removal of one entire M$_3$O$_{13}$ triad.

(14) Nomiya, K.; Arai, Y.; Shimizu, Y.; Takahashi, M.; Takayama, T.; Weiner, H.; Nagata, T.; Widegren, J. A.; Finke, R. G. *Inorg. Chim. Acta* **2000**, *300−302*, 285−304.

(15) Lyons, J. E.; Ellis, P. E., Jr.; Langdale, W. A.; Myers, H. K., Jr. Method of Preparing Heteropolyacid Catalysts. U.S. Patent 4,916,101, Apr 10, 1990.

(16) Mizuno, N.; Hirose, T.; Tateishi, M.; Iwamoto, M. *J. Mol. Catal.* **1994**, *88*, L125−L131.

(17) (a) Jun, P.; Lunyu, Q.; Yaguang, C. *Inorg. Chim. Acta* **1991**, *183*, 157−160. (b) Lihua, B.; Jun, P.; Yaguang, C.; Jingfu, L.; Lunyu, Q. *Polyhedron* **1994**, *13*, 2421−2424.

(18) (a) Wassermann, K.; Lunk, H. J.; Palm, R.; Fuchs, J. *Acta Crystallogr., Sect. C* **1994**, *50*, 348−350. (b) Coronado and co-workers reported a trisubstituted structure ((NiOH$_2$)$_3$PW$_{10}$O$_{39}$$^{7-}$), but it also contained an additional WO$_6$ octahedron capping the three edge-sharing NiO$_6$ octahedra. See: Gómez-García, C. J.; Coronado, E.; Ouahab, L. *Angew. Chem., Int. Ed. Engl.* **1992**, *31*, 649−651.

(19) (a) Lunyu, Q.; Yingji, S.; Yanguang, C.; Ming, Y.; Jun, P. *Synth. React. Inorg. Met.-Org. Chem.* **1994**, *24*, 1339−1350. (b) Liu, J. F.; Zhang, X. P.; Chen, Y. G.; Li, G. P.; Wang, J. P. *Transition Met. Chem. (London)* **1995**, *20*, 327−329 and references therein.

(20) Meng, L.; Zhan, X.-P.; Wang, M.; Liu, J.-F. *Polyhedron* **2001**, *20*, 881−885.

(21) Knoth, W. H.; Domaille, P. J.; Farlee, R. D. *Organometallics* **1985**, *4*, 62−68.

(22) Knoth, W. H.; Domaille, P. J.; Harlow, R. L. *Inorg. Chem.* **1986**, *25*, 1577−1584.

(23) Finke, R. G.; Rapko, B.; Weakley, T. J. R. *Inorg. Chem.* **1989**, *28*, 1573−1579.

(24) (a) Craciun, C.; David, L.; Rusu, D.; Rusu, M.; Cozar, O.; Marcu, G. *J. Radioanal. Nucl. Chem.* **2001**, *247*, 307−310. (b) Rusu, D.; Craciun, C.; Barra, A.-L.; David, L.; Rusu, M.; Rosu, C.; Cozar, O.; Marcu, G. *J. Chem. Soc., Dalton Trans.* **2001**, 2879−2887. (c) Rusu, D.; Rosu, C.; Craciun, C.; David, L.; Rusu, M.; Marcu, G. *J. Mol. Struct.* **2001**, *563−564*, 427−433.

(25) (a) Mialane, P.; Marrot, J.; Rivière, E.; Nebout, J.; Hervé, G. *Inorg. Chem.* **2001**, *40*, 44−48. (b) Kortz, U.; Al-Kassem, N. K.; Savelieff, M. G.; Al Kadi, N. A.; Sadakane, M. *Inorg. Chem.* **2001**, *40*, 4742−4749.

(26) References 24 and 25 represent a distinct subclass of sandwich-type POMs where three square pyramidal MO$_5$ units are sandwiched between two B-type α-XW$_9$O$_{33}$$^{n-}$ units (formula (MOH$_2$)$_3$(B-α-XW$_9$O$_{33}$)$_2$$^{9-}$, where M = 3d metal and X = As(III), Bi(III), or Sb(III)).

(27) Weakley, T. J. R.; Evans, H. T., Jr.; Showell, J. S.; Tourné, G. F.; Tourné, C. M. *J. Chem. Soc., Chem. Commun.* **1973**, *4*, 139−140.

(28) Finke, R. G.; Droege, M.; Hutchinson, J. R.; Gansow, O. *J. Am. Chem. Soc.* **1981**, *103*, 1587−1589.

(29) Finke, R. G.; Droege, M. W. *Inorg. Chem.* **1983**, *22*, 1006−1008.

(30) Evans, H. T.; Tourné, C. M.; Tourné, G. F.; Weakley, T. J. R. *J. Chem. Soc., Dalton Trans.* **1986**, 2699−2705.

(31) Wasfi, S. H.; Rheingold, A. L.; Kokoszka, G. F.; Goldstein, A. S. *Inorg. Chem.* **1987**, *26*, 2934−2939.

(32) Finke, R. G.; Droege, M. W.; Domaille, P. J. *Inorg. Chem.* **1987**, *26*, 3886−3896.

(33) Tourné, C. M.; Tourné, G. F.; Zonnevijlle, F. *J. Chem. Soc., Dalton Trans.* **1991**, 143−155.

(34) Casañ-Pastor, N.; Bas-Serra, J.; Coronado, E.; Pourroy, G.; Baker, L. C. W. *J. Am. Chem. Soc.* **1992**, *114*, 10380−10383.

(35) (a) Reference 18b. (b) Gómez-García, C. J.; Coronado, E.; Gómez-Romero, P.; Casañ-Pastor, N. *Inorg. Chem.* **1993**, *32*, 89−93. (c) Gómez-García, C. J.; Coronado, E.; Gómez-Romero, P.; Casañ-Pastor, N. *Inorg. Chem.* **1993**, *32*, 3378−3381. (d) Clemente, J. M.; Coronado, E.; Galán-Mascarós, J. R.; Gómez-García, C. J. *Inorg. Chem.* **1999**, *38*, 55−63.

(36) Zhang, X.-Y.; O'Connor, C. J.; Jameson, G. B.; Pope, M. T. *Inorg. Chem.* **1996**, *35*, 30−34.

(37) Weakley, T. J. R.; Finke, R. G. *Inorg. Chem.* **1990**, *29*, 1235−1241.

(38) Khenkin, A. M.; Hill, C. L. *Mendeleev Commun.* **1993**, 140−141.

(39) Gómez-García, C. J.; Borrás-Almenar, J. J.; Coronado, E.; Ouahab, L. *Inorg. Chem.* **1994**, *33*, 4016−4022.

(40) Finke, R. G.; Weakley, T. J. R. *J. Chem. Crystallogr.* **1994**, *24*, 123−128.

(41) Zhang, X.; Chen, Q.; Duncan, D. C.; Campana, C.; Hill, C. L. *Inorg. Chem.* **1997**, *36*, 4208−4215.

(42) Zhang, X.; Chen, Q.; Duncan, D. C.; Lachicotte, R. J.; Hill, C. L. *Inorg. Chem.* **1997**, *36*, 4381−4386.

(43) Rusu, M.; Marcu, G.; Rusu, D.; Rosu, C.; Tomsa, A.-R. *J. Radioanal. Nucl. Chem.* **1999**, *242*, 467−472.

(44) Bi, L. H.; Wang, E.-B.; Peng, J.; Huang, R. D.; Xu, L.; Hu, C. W. *Inorg. Chem.* **2000**, *39*, 671−679.

(45) Kortz, U.; Isber, S.; Dickman, M. H.; Ravot, D. *Inorg. Chem.* **2000**, *39*, 2915−2922.

Figure 2. Wireframe representations of the structures discussed in this paper (with junctions labeled as α or β). The central units of the sandwich-type structures are shown in combination polyhedral/ball-and-stick representation. **1** or **2**: α-(FeL)$_3$P$_2$W$_{15}$O$_{59}$$^{n-}$ (where L = Cl$^-$ or H$_2$O). **3**: αββα-(Fe^{III}OH$_2$)$_2$-Fe^{III}$_2$(P$_2$W$_{15}$O$_{56}$)$_2$$^{12-}$. **4**: ααβα-(NaOH$_2$)(Fe^{III}OH$_2$)Fe^{III}$_2$(P$_2W_{15}O_{56}$)$_2$$^{14-}$. **5**: αααα-(NaOH$_2$)$_2Fe^{III}_2$(P$_2W_{15}O_{56}$)$_2$$^{16-}$. **6**: αββα-(Ni^{II}OH$_2$)$_2Fe^{III}_2$(P$_2W_{15}O_{56}$)$_2$$^{14-}$. **7**: ααβα-(Cu^{II}OH$_2$)Fe^{III}$_2$(P$_2W_{15}O_{56}$)(P$_2Cu^{II}_2$(OH$_2$)$_4W_{13}O_{52}$)$^{16-}$.

have suggested three possible reasons.[32] First, there is often a significant difference in the size of a low-valent d-electron-containing transition metal cation and the size of the "hole" in the POM unit previously occupied by a high-valent metal such as W^{VI}.[53] The larger d-electron-containing metal centers might be better accommodated by sandwich-type structures because they effectively form a M$_4$O$_{14}$(OH$_2$)$_2$ group encapsulated between two trivacant POM units. The M$_4$O$_{14}$(OH$_2$)$_2$ group fills the void left by the missing M$_3$O$_{13}$ units without the incorporation of three new metal centers per trivacant POM (i.e., two metal sites are shared between the two trivacant POM subunits). Second, there is an increase in the overall charge of the POM (and therefore increased basicity) due to the lower charge of the incoming cation ([Co(OH$_2$)]$^{2+}$ replacement of (W=O)$^{4+}$, for example). In this context,

reaction of α-P$_2$W$_{15}$O$_{56}$$^{12-}$ with M(III) could yield either (M^{III}OH$_2$)$_2$(M^{III})$_2$(P$_2$W$_{15}$O$_{56}$)$_2$$^{12-}$ or α-P$_2$(M^{III}OH$_2$)$_3$W$_{15}$O$_{59}$$^{9-}$, but the sandwich-type POM has a lower negative charge (per POM unit) than the parent structure, α-P$_2$(M^{III}OH$_2$)$_3$W$_{15}$O$_{59}$$^{9-}$. Because the formation of POMs is kinetically controlled, the product with a lower negative charge is often favored.[54] Third, thermodynamic factors appear to favor the sandwich-type structures over the trisubstituted parent species (previous reports suggest that sandwich-type POMs are more thermodynamically stable than their monomeric Wells−Dawson and Keggin counterparts).[32,41,42,46,55,56]

All previously known sandwich-type POMs derived from trivacant Wells−Dawson and B-Keggin units with one exception have β-junctions between the trivacant species and the central M$_4$ unit (Figure 2).[27−45,47] The exception is the complex, αααα-(NaOH$_2$)$_2$Fe^{III}$_2$(P$_2$W$_{15}$O$_{56}$)$_2$$^{16-}$, that has α-junc-

(46) Zhang, X.; Anderson, T. M.; Chen, Q.; Hill, C. L. *Inorg. Chem.* **2001**, *40*, 418−419.
(47) Bi, L. H.; Huang, R. D.; Peng, J.; Wang, E.-B.; Wang, Y.-H.; Hu, C.-W. *J. Chem. Soc., Dalton Trans.* **2001**, 121−129.
(48) (a) Li, M.-X.; Jin, S.-L.; Liu, H.-Z.; Xie, G.-Y., Chen, M.-Q.; Xu, Z.; You, X.-Z. *Polyhedron* **1998**, *17*, 3721−3725. (b) Kortz, U.; Savelieff, M. G.; Bassil, B. S.; Keita, B.; Nadjo, L. *Inorg. Chem.* **2002**, *41*, 783−789 and references therein.
(49) Lin, Y.; Weakley, T. J. R.; Rapko, B.; Finke, R. G. *Inorg. Chem.* **1993**, *32*, 5095−5101.
(50) Keita, B.; Mbomekalle, I. M.; Nadjo, L.; Contant, R. *Electrochem. Commun.* **2001**, *3*, 267−273.
(51) Wassermann, K.; Palm, R.; Lunk, H.-J.; Fuchs, J.; Steinfeldt, N.; Stösser, R. *Inorg. Chem.* **1995**, *34*, 5029−5036 and references therein.
(52) Harmalker, S. P.; Leparulo, M. A.; Pope, M. T. *J. Am. Chem. Soc.* **1983**, *105*, 4286−4292.
(53) For example, the radius of octahedrally coordinated W^{VI} is 0.74 Å, while that of high-spin octahedral Co^{II} is 0.885 Å.

(54) (a) POMs of higher charge are not necessarily less stable than the POMs of lower charge, but current data suggest that in the formation of new POMs (from other preformed POMs) the species with a lower negative charge is the more favorable product. This concept is used to partially explain why alkaline degradation of β$_2$-SiW$_{11}$O$_{39}$$^{8-}$ yields γ-SiW$_{10}$O$_{36}$$^{8-}$ instead of β-SiW$_{10}$O$_{37}$$^{10-}$. See Canny, J.; Tézé, A.; Thouvenot, R.; Hervé, G. *Inorg. Chem.* **1986**, *25*, 2114−2119. (b) Another explanation for the dominating force towards dimerization is the reduction in the number of terminal water (aqua) ligands per Fe(III) center. The kinetic stability observed (i.e., **4** > **3** > **5** > **1** or **2**) does not follow this trend exactly, but this may be attributed to structural differences as well. We thank an anonymous reviewer for bringing this to our attention.
(55) Neumann, R.; Gara, M. *J. Am. Chem. Soc.* **1994**, *116*, 5509−5510.
(56) Previous reports note that prolonged heating of A-α-X(MOH$_2$)$_3$W$_9$O$_{37}$$^{n-}$ results in the formation of sandwich-type structures. See references 12 and 22.

tions between the trivacant POM units and a unique M_2 central unit.[46] Because the Na centers are weakly bonded and labile, this complex is effectively a lacunary sandwich-type POM. Incorporation of one Cu(II) or Co(II) ion into the central unit of this complex yields a structure with one α-junction and one β-junction between the trivacant POM units and a new central M_3 unit.[57,58] The predominance of the central β-junction over the α-junction in sandwich-type POMs is opposite the known relative thermodynamic stabilities of α versus β isomers in the parent Wells−Dawson and Keggin structures.[59] These energy differences have been attributed to possible steric interactions between the coordinated water ligands of the external metal sites (of the central multimetal unit) and the bridging oxygen atoms of the neighboring belt tungsten atoms.[32]

We now report the Fe^{III}_3 capped Wells−Dawson complex, α-$(Fe^{III}Cl)_2(Fe^{III}OH_2)P_2W_{15}O_{59}^{11-}$ (**1**). This is the first example of a monomeric Wells−Dawson structure trisubstituted with low-valent transition metals (i.e., valency <4). There are several reports of trisubstituted Keggin derivatives of formula $X(MOH_2)_3W_9O_{37}^{n-}$, but complete X-ray crystallographic structure determination of many of these complexes has remained elusive.[12,14−20] One notable exception is the structurally characterized complex A-α-$Si(CrOH_2)_3W_9O_{37}^{7-}$.[18] This paper first addresses the syntheses of α-$(Fe^{III}Cl)_2(Fe^{III}-OH_2)P_2W_{15}O_{59}^{11-}$ (**1**) and α-$(Fe^{III}OH_2)_3P_2W_{15}O_{59}^{9-}$ (**2**) from isomerically pure α-$P_2W_{15}O_{56}^{12-}$ and Fe(III) in a saturated NaCl solution. The complexes are fully characterized by ^{31}P NMR, IR, elemental analysis, and, most significantly, X-ray crystallography (Figure 2). At low ionic strength values (<1 M), **1** decomposes to form the traditional sandwich-type POM αββα-$(Fe^{III}OH_2)_2Fe^{III}_2(P_2W_{15}O_{56})_2^{12-}$ (**3**),[60] or a new sandwich-type isomer, ααβα-$(NaOH_2)(Fe^{III}OH_2)Fe^{III}_2(P_2-W_{15}O_{56})_2^{14-}$ (**4**), depending on the pH of the solution. The new complex, **4**, is also obtained as a byproduct in the synthesis of αααα-$(NaOH_2)_2Fe^{III}_2(P_2W_{15}O_{56})_2^{16-}$ (**5**). To probe the role of the external metal sites of the central junction in both formation and stability (i.e., susceptibility to degradation at high temperature and pH) of these sandwich-type POMs, we have prepared a new mixed-metal derivative, αββα-$(Ni^{II}OH_2)_2Fe^{III}_2(P_2W_{15}O_{56})_2^{14-}$ (**6**), by reacting **5** with an excess of Ni(II). Unlike the reaction of **5** with Cu(II) or Co(II), two metal centers are incorporated into the central unit without additional substitution of $α_1$ (belt) tungstens in the α-$P_2W_{15}O_{56}^{12-}$ units. With the full characterization of these four new structures (along with data on

catalysis of H_2O_2-based epoxidation), trends in the formation and stability of POMs based on trivacant Wells−Dawson units as a function of ionic strength, pH, and the intrinsic Jahn−Teller distortion of the incorporated metal are proposed (Figure 2).

Experimental Section

General Methods and Materials. α-$Na_{12}[P_2W_{15}O_{56}]\cdot18H_2O$ was synthesized according to literature procedures.[32,61] Br, Cl, Fe, Na, Ni, P, and W analyses were performed by Desert Analytics Laboratory in Tucson, AZ. C, H, and N analyses were performed by Atlantic Microlab Inc. in Norcross, GA. Infrared spectra (2% sample in KBr) were recorded on a Nicolet 510 FTIR instrument. The electronic absorption spectra were taken on a Hewlett-Packard 8452A UV−vis spectrophotometer. ^{31}P NMR measurements were made on a Varian INOVA 400 MHz spectrometer, and peaks were referenced to 85% H_3PO_4. Average magnetic susceptibilities were measured on a Johnson Matthey Model MSB-1 magnetic susceptibility balance as neat powders at 24 °C; the balance was calibrated using $Hg[Co(SCN)_4]$ as a standard. Pascal's constants were used to obtain the final diamagnetic corrections.

Synthesis of α-$Na_{11}[(FeCl)_2(FeOH_2)P_2W_{15}O_{59}]\cdot14H_2O$ (Na1). Ferric chloride hexahydrate (1.2 g, 4.5 mmol) was dissolved in 14 mL of 4 M NaCl solution, and α-$Na_{12}[P_2W_{15}O_{56}]$ (6 g, 1.5 mmol) was added slowly with vigorous stirring. The solution was stirred for 10 min at room temperature and was filtered with a medium porosity (glass-sintered) frit. The solution was cooled to 10 °C overnight, and large orange crystals were collected and redissolved in 10 mL of 1.5 M NaCl. Diffraction quality crystals were formed after several days. (2.6 g, yield 40%). IR (2% KBr pellet, 1300−400 cm^{-1}): 1086 (s), 1014 (w), 942 (s), 905 (m), 812 (s), 698 (w), 574 (w), 558 (w), 524 (m), 479 (w), and 432 (w). ^{31}P NMR (15 mM POM, in D_2O saturated in NaCl): one peak for the distal P atom at −15.8 ppm ($\Delta\nu_{1/2}$ = 60 Hz). Magnetic susceptibility: μ_{eff} = 7.9 μ_B/mol at 297 K. Anal. Calcd for $H_{30}Cl_2Fe_3Na_{11}O_{74}P_2W_{15}$: Cl, 1.57; Fe, 3.70; Na, 5.59; P, 1.37; W, 60.94. Found: Cl, 1.52; Fe, 3.74; Na, 5.46; P, 1.41; W, 60.97. [MW = 4525.2.]

Synthesis of α-$Na_9[(FeOH_2)_3P_2W_{15}O_{59}]\cdot19H_2O$ (Na2). Complex **1** (1 g, 0.23 mmol) was dissolved in 30 mL of 1 M NaBr with vigorous stirring. Yellow-orange cubic crystals were formed after several days (0.65 g, yield 65%). IR (2% KBr pellet, 1300−400 cm^{-1}): 1090 (s), 1013 (w), 950 (s), 893 (m), 807 (s), 727 (m), 638 (w), 623 (w), 524 (m), 477 (w), and 422 (w). ^{31}P NMR (15 mM solution in D_2O): one peak for the distal P atom at −16.4 ppm ($\Delta\nu_{1/2}$ = 75 Hz). Magnetic susceptibility: μ_{eff} = 7.9 μ_B/mol at 297 K. Anal. Calcd for $H_{44}Br_0Fe_3Na_9O_{81}P_2W_{15}$: Br, 0.00; Fe, 3.69; Na, 4.56; P, 1.37; W, 60.82. Found: Br, 0.00; Fe, 3.74; Na, 4.45; P, 1.40; W, 60.77. [MW = 4534.4.]

Synthesis of $Na_{14}[ααβα-(NaOH_2)(FeOH_2)Fe_2(P_2W_{15}O_{56})_2]\cdot20H_2O$ (Na4). Solid α-$Na_{12}[P_2W_{15}O_{56}]$ (5 g, 1.25 mmol) was slowly added (with stirring) to ferrous chloride tetrahydrate (0.49 g, 2.46 mmol) dissolved in 30 mL of 1 M NaCl. The solution was heated gently at 65 °C for 5−10 min, filtered hot, and the filtrate cooled to 10 °C. Dark green crystals[62] that formed overnight were redissolved in 30 mL of H_2O and allowed to oxidize in air for 5 days at ambient temperature. Each day, solid Fe_2O_3 (identified by elemental analysis) was removed by centrifugation. Sodium chloride (1.5 g) was added, and the solution was stirred for 10−15 min. A yellow-brown precipitate was removed using a 0.45 μm (pore size)

(57) Anderson, T. M.; Hardcastle, K. I.; Okun, N.; Hill, C. L. *Inorg. Chem.* **2001**, *40*, 6418−6425.

(58) This structure also has two additional Cu(II) or Co(II) atoms in one of the two Wells−Dawson units (in $α_1$ sites). See structure **7** in Figure 2.

(59) Quantitative determinations of energy differences for the α and β isomers of Keggin and Wells−Dawson POMs under equilibrium conditions were recently reported. See: (a) Weinstock, I. A.; Cowan, J. J.; Barbuzzi, E. M. G.; Zeng, H.; Hill, C. L. *J. Am. Chem. Soc.* **1999**, *121*, 4608−4617. (b) Anderson, T. M.; Hill, C. L. *Inorg. Chem.*, in submission.

(60) αββα is used in the sandwich-type structures to indicate the connectivity for the first cap-belt junction, the first and second belt-central M_4 junctions, and the second belt-cap junctions, respectively (Figure 2).

(61) Contant, R. In *Inorganic Syntheses*; Ginsberg, A. P., Ed.; John Wiley and Sons: New York, 1990; Vol. 27, pp 104−111.

microfilter, and the yellow-orange filtrate was left exposed to the air. After 1−2 days, large light-yellow plates formed and were collected on a medium frit. This product has been previously identified as $\alpha\alpha\alpha\alpha$-(NaOH$_2$)$_2$Fe$^{III}_2$(P$_2$W$_{15}$O$_{56}$)$_2^{16-}$.[46] The filtrate was concentrated to approximately 70% of its original volume, and a light yellow precipitate was collected. This compound was recrystallized from 0.5 M NaCl (3.7 g, yield 70%). IR (2% in KBr pellet, 1300−400 cm^{-1}): 1089 (s), 1053 (m, sh), 1018 (w), 946 (m), 918 (w), 881 (w), 834 (w), 745 (m), 699 (m), 597 (w), and 515 (w). ^{31}P NMR (15 mM solution in D$_2$O): two peaks for two symmetry inequivalent distal P atoms at −11.9 ($\Delta\nu_{1/2}$ = 75 Hz) and −14.5 ppm ($\Delta\nu_{1/2}$ = 200 Hz). Magnetic susceptibility: μ_{eff} = 8.5 μ_B/mol at 297 K. Anal. Calcd for H$_{44}$Fe$_3$Na$_{15}$O$_{134}$P$_4$W$_{30}$: Fe, 2.01; Na, 4.13; P, 1.49; W, 66.13. Found: Fe, 2.09; Na, 4.16; P, 1.48; W, 65.41. [MW = 8340.1.]

Synthesis of [(CH$_3$CH$_2$CH$_2$CH$_2$)$_4$N]$_{15}$[$\alpha\alpha\beta\alpha$-Fe$_3$(P$_2$W$_{15}$O$_{56}$)$_2$] (TBA4). The tetra-*n*-butylammonium (TBA) salt of **4** was prepared by a metathesis reaction. To 1.0 g (0.12 mmol) of Na**4** in 30 mL of H$_2$O was added with stirring 0.50 g (1.8 mmol) of TBACl. CH$_2$-Cl$_2$ (250 mL) was added to this cloudy solution, and the mixture was shaken in a separatory funnel. After standing for 30 min, the mixture separated into a cloudy colorless upper layer and a clear yellow lower layer. The bottom organic layer was collected and concentrated to a thick oil with a rotary evaporator. A yellow solid was then precipitated from the concentrated organic layer by addition of diethyl ether (∼100 mL). The resulting solid was collected on a medium frit and dried under vacuum for 24 h (1.2 g, yield 80%). IR and elemental analysis establish that **4** had not changed during the conversion of Na**4** to TBA**4**. IR (2% KBr pellet, 1300−400 cm^{-1}): 1151 (m), 1087 (s), 1049 (m, sh), 1014 (w), 947 (s), 911 (m), 887 (m), 834 (m), 746 (m), 697 (m), 598 (w), and 499 (w). Anal. Calcd for C$_{240}$H$_{540}$Fe$_3$N$_{15}$O$_{112}$P$_4$W$_{30}$: C, 25.47; H, 4.81; Fe, 1.48; N, 1.86; P, 1.09; W, 48.74. Found: C, 25.43; H, 4.77; Fe, 1.46; N, 1.83; P, 1.12; W, 49.01. [MW = 11235.9.]

Synthesis of Na$_{14}$[$\alpha\beta\beta\alpha$-(NiOH$_2$)$_2$Fe$_2$(P$_2$W$_{15}$O$_{56}$)$_2$]·24H$_2$O (Na6) and [(CH$_3$CH$_2$CH$_2$CH$_2$)$_4$N]$_{14}$[$\alpha\beta\beta\alpha$-Ni$_2$Fe$_2$(P$_2$W$_{15}$O$_{56}$)$_2$] (TBA6). The parent diferric complex **5** (0.750 g, 0.0825 mmol) was dissolved in a minimal amount of 0.5 M NaCl, and the pH was adjusted to ∼2 by addition of HCl. NiCl$_2$·6H$_2$O (0.320 g, 0.825 mmol) was slowly added and the resulting solution heated to 60 °C for ∼10 min. The solution color changed slightly (from greenish-yellow to dark yellow) on heating. After ∼7 days, a yellow precipitate formed that was recrystallized from 0.25 M NaCl (0.46 g, yield 66%). IR (2% KBr pellet, 1300−400 cm^{-1}): 1086 (s), 1060 (w, sh), 1017 (w, sh), 945 (s), 927 (m), 876 (m), 837 (m), 788 (s), 747 (m), 702 (s), 518 (m), and 487 (w). ^{31}P NMR (9 mM solution in D$_2$O): −16.9 ppm, $\Delta\nu_{1/2}$ = 300 Hz. Magnetic susceptibility: μ_{eff} = 10.3 μ_B/mol at 297 K. Anal. Calcd for H$_{48}$Fe$_2$Na$_{14}$Ni$_2$O$_{138}$P$_4$W$_{30}$: Fe, 1.32; Na, 3.81; Ni, 1.39; P, 1.47; W, 65.30. Found: Fe, 1.36; Na, 3.85; Ni, 1.36; P, 1.45; W, 64.82. [MW = 8446.6.] The tetra-*n*-butylammonium salt was prepared by treating 0.4 g of Na**6** in 25 mL of H$_2$O with 0.16 g TBACl followed by extraction with 150 mL of CH$_2$-Cl$_2$. Addition of Et$_2$O to the green lower organic layer afforded 0.38 g (∼80% yield). IR (2% KBr pellet, 1300−400 cm^{-1}): 1106 (w), 1087 (s), 1049 (w, sh), 1014 (w, sh), 947 (s), 911 (m), 888 (m), 824 (m), 786 (m), 749 (w), 696 (s), 528 (m), and 480 (w). Anal. Calcd for C$_{144}$H$_{504}$Fe$_2$N$_{14}$Ni$_2$O$_{112}$P$_4$W$_{30}$: C, 17.13; H, 5.03;

Fe, 1.11; N, 1.94; Ni, 1.16; P, 1.23; W, 54.64. Found: C, 16.99; H, 5.08; Fe, 1.19; N, 2.02; Ni, 1.19; P, 1.16; W, 53.82. [MW = 10126.1.]

X-ray Crystallography. Suitable crystals of Na**1**, Na**2**, Na**4**, and Na**6** were coated with Paratone N oil, suspended on a small fiber loop, and placed in a cooled nitrogen stream at 100 K on a Bruker D8 SMART APEX CCD sealed tube diffractometer with graphite monochromated Mo Kα (0.71073 Å) radiation. A sphere of data was measured using a series of combinations of ϕ and ω scans with 10 s frame exposures and 0.3° frame widths. Data collection, indexing, and initial cell refinements were all handled using SMART software.[63a] Frame integration and final cell refinements were carried out using SAINT software.[63b] The final cell parameters were determined from least-squares refinement. The SADABS program was used to carry out absorption corrections.[64a]

The structure was solved using direct methods and difference Fourier techniques (SHELXTL, V5.10).[64b] All atoms were refined anisotropically, except where noted (see Supporting Information).[65] The final R1 scattering factors and anomalous dispersion corrections were taken from the *International Tables for X-ray Crystallography*.[66] Structure solution, refinement, graphics, and generation of publication materials were performed by using SHELXTL, V5.10 software.[64b] Additional details of data collection and structure refinement are given in Table 1, and thermal ellipsoid plots (at the 50% probability level) are given in Figure 3. Disorder of the Na atoms prevented the identification (crystallographically) of all Na$^+$ countercations in the four structures.

Catalytic Oxidation of Alkenes. In each reaction, the alkene substrate (0.9 mmol) and TBA**4** or TBA**6** (0.004 mmol) were stirred under Ar at 25 °C in 1 mL of CH$_3$CN in a 10-mL Schlenk flask fitted with a Teflon stopcock and rubber stopper. The reaction was initiated by the addition of 25 μL of 30% aqueous H$_2$O$_2$. The organic products were identified and quantified by GC/MS and GC, respectively, using decane as the internal standard. The final H$_2$O$_2$ concentration was measured using standard iodometric analyses.[67]

Thermal Stability Experiments. Solutions of **3−5** (0.09 M) were adjusted to common pH values (ranging from 3.0 to 5.7) by addition of 1 M HCl or 1 M NaOH and placed in glass vials with sealed caps. The ionic strength was adjusted by adding appropriate quantities of LiCl, NaCl, KCl, or NH$_4$Cl. The solutions were degassed as liquids and purged with Ar. The vials were heated in a mineral oil bath at various temperatures (from 20 to 80 °C) and the contents stirred magnetically at a constant speed of 200 rpm. Aliquots (0.7 mL) were removed from the vials at measured time intervals, immediately cooled to ambient temperature, and then analyzed by ^{31}P NMR.

Results and Discussion

Syntheses. The preparation of α-(Fe^{III}Cl)$_2$(Fe^{III}OH$_2$)-P$_2$W$_{15}$O$_{59}^{11-}$ (**1**) is very similar to the preparation of the

(62) The dark green crystals formed in the synthesis of Na**4** are Na$_{16}$[(Fe^{II}-OH$_2$)$_2$Fe$^{II}_2$(P$_2$W$_{15}$O$_{56}$)$_2$] (the Fe/P/W ratios from elemental analysis are 2/2/15, and the IR spectrum is virtually identical to that of Na$_{16}$[(ZnOH$_2$)$_2$Zn$_2$(P$_2$W$_{15}$O$_{56}$)$_2$]). See reference 46.

(63) (a) *SMART*, version 5.55; Bruker AXS, Inc., Madison, WI, 2000. (b) *SAINT*, version 6.02; Bruker AXS, Inc., Madison, WI, 1999.

(64) (a) Sheldrick, G. *SADABS*; University of Göttingen: Göttingen, Germany, 1996. (b) *SHELXTL*, version 5.10; Bruker AXS, Inc.: Madison, WI, 1997.

(65) For Na**1**, all Fe, W, Na, and Cl atoms were refined anisotropically. For Na**2**, only W and Na atoms were refined anisotropically. For Na**4**, only W, Fe, P, and Na atoms (as well as water oxygen atoms) were refined anisotropically. For Na**6**, all W, Fe, Na, and Ni and all but O1s, O11s, and O12s of the water oxygen atoms were refined anisotropically. Crystal quality was the limiting factor for determining which atoms were refined anisotropically.

(66) *International Tables for X-ray Crystallography*; Kynoch Academic Publishers: Dordrecht, Netherlands, 1992; Vol. C.

(67) Day, R. A., Jr.; Underwood, A. L. *Quantitative Analysis*, 5th ed.; Prentice Hall: Englewood Cliffs, NJ, 1986.

Table 1. Crystal Data and Structure Refinement for Na**1**, Na**2**, Na**4**, and Na**6**

	Na**1**	Na**2**	Na**4**	Na**6**
empirical formula	$Cl_2Fe_3Na_6O_{88}P_2W_{15}$	$Fe_3Na_8O_{81}P_2W_{15}$	$Fe_3Na_{11}O_{144}P_4W_{30}$	$H_{52}Fe_2Na_5Ni_2O_{138}P_4W_{30}$
fw	4602.36	4455.7	8344.33	8243.9
cryst syst	monoclinic	triclinic	triclinic	triclinic
space group	$P2_1/n$	$P1$	$P\bar{1}$	$P\bar{1}$
unit cell	$a = 13.343(2)$ Å	$a = 12.859(1)$ Å	$a = 13.797(1)$ Å	$a = 13.781(2)$ Å
	$b = 28.535(3)$ Å	$b = 13.349(1)$ Å	$b = 22.051(1)$ Å	$b = 13.878(2)$ Å
	$c = 21.574(2)$ Å	$c = 22.250(2)$ Å	$c = 24.594(2)$ Å	$c = 21.444(3)$ Å
	$\alpha = 90°$	$\alpha = 92.471(2)°$	$\alpha = 109.949(2)°$	$\alpha = 91.553(2)°$
	$\beta = 92.139(2)°$	$\beta = 97.309(2)°$	$\beta = 99.041(2)°$	$\beta = 96.024(2)°$
	$\gamma = 90°$	$\gamma = 108.181(2)°$	$\gamma = 93.748(2)°$	$\gamma = 118.480(2)°$
V	$8208.3(2)$ Å^3	$3585.4(5)$ Å^3	$6888.8(6)$ Å^3	$3571.0(8)$ Å^3
Z/density (calcd)	4/3.724 Mg/m^3	2/4.127 Mg/m^3	2/4.023 Mg/m^3	1/3.833 Mg/m^3
abs coeff	21.695 mm^{-1}	24.755 mm^{-1}	25.433 mm^{-1}	24.667 mm^{-1}
reflns collected	146867	61769	106050	40806
indep reflns	29048 [R(int) = 0.1839]	46442 [R(int) = 0.0418]	27027 [R(int) = 0.0770]	12184 [R(int) = 0.1063]
GOF on F^2	1.069	0.927	1.285	1.117
final R indices [$I > 2\sigma(I)$]	R1^a = 0.0679	R1^a = 0.0483	R1^a = 0.0900	R1^a = 0.0800
	wR2^b = 0.2351	wR2^b = 0.0789	wR2^b = 0.1834	wR2^b = 0.1852

^{a} R1 $= \Sigma||F_o| - |F_c||/\Sigma|F_o|$. ^{b} wR2 $= \{\Sigma[w(F_o^2 - F_c^2)^2]/\Sigma[w(F_o^2)^2]\}^{0.5}$.

tetraferric sandwich-type POM, $\alpha\beta\beta\alpha$-(Fe^{III}OH$_2$)$_2$Fe^{III}$_2$-(P$_2$W$_{15}$O$_{56}$)$_2$$^{12-}$ (**3**), with three exceptions (see Figure 2 for general structures). First, a 3:1 ratio of Fe(III) to α-P$_2$W$_{15}$O$_{56}$$^{12-}$ is used (a 2:1 ratio was used in the preparation of the tetraferric sandwich). Second, **1** is synthesized at ambient temperature while the sandwich-type POM (**3**) was heated to 80 °C. Third, **1** is prepared in aqueous media of significantly higher ionic strength (the concentration of NaCl is 4 M versus 1 M for the tetraferric sandwich). Once the complex is prepared, it is only stable in solutions at least 1 M in NaCl. Solutions of lower ionic strength always result in decomposition, as confirmed by ^{31}P NMR. The high ionic strength necessary to stabilize **1** does not allow isolation of the tetra-*n*-butylammonium salt. Complex **2** (α-(Fe^{III}-OH$_2$)$_3$P$_2$W$_{15}$O$_{59}$$^{9-}$) is prepared by dissolving **1** in a 1 M solution of NaBr. The ionic strength of this solution is high enough to prevent decomposition, while simultaneously allowing the two terminal Cl$^-$ ligands on the Fe^{III}$_3$ cap to be exchanged for water (aqua) ligands. No coordination of **2** with Br$^-$ is observed. This was confirmed by elemental analysis and by X-ray diffraction analysis.

Complex **1** has two peaks in the solution ^{31}P NMR spectrum. This could be consistent with two P atoms that are not symmetry equivalent, but in all previously reported Fe(III)−POM structures, the peaks due to the P atoms proximal to an Fe(III) site are usually not observed.[41,46] However, one of the two peaks in the ^{31}P NMR spectrum of **1** was identified by comparison with an authentic sample of **2** (-16.4 ppm). In addition, the ratio of the integrated areas of the two peaks is found to be dependent on the NaCl concentration of the solution (Figure 4). At high NaCl concentration, the peak assigned to **2** completely disappears. The single peak remaining was then assigned to complex **1** (-15.8 ppm).[68] The IR spectra of Na**1** and Na**2** are similar to the parent complex, α-P$_2$W$_{18}$O$_{62}$$^{6-}$. Both complexes have

terminal W−O stretching and W−O−W bridging bands characteristic of heteropolytungstates.[69] There is no splitting observed in the υ_3 vibrational mode of the central PO$_4$ units.

At low concentrations of NaCl (<1 M), **1** reacts with itself to form the tetraferric sandwich-type complex, **3**. Polyanion **3** can be isolated in solution or as a solid. In solution, **3** can be converted back to **1**, however, when additional NaCl is added, and the solution is heated for approximately 1 h at 75 °C. These observations suggest the overall charge of the complex may affect (at least in part) whether the sandwich-type structure or the parent Wells−Dawson structure is the product, because the monomeric species (**1** or **2**) both have a higher charge (per POM unit) than the sandwich-type structure (**3**).[70] If the pH is higher than 5, a new triferric sandwich-type complex, $\alpha\alpha\beta\alpha$-(NaOH$_2$)(Fe^{III}OH$_2$)Fe^{III}$_2$-(P$_2$W$_{15}$O$_{56}$)$_2$$^{14-}$ (**4**), is formed instead of **3** (see Figure 2 for general structures). Complex **4** may also be isolated (as a solid) in high yield ($\sim$70%) during the synthesis of the diferric sandwich-type complex, $\alpha\alpha\alpha\alpha$-(NaOH$_2$)$_2$Fe^{III}$_2$-(P$_2$W$_{15}$O$_{56}$)$_2$$^{16-}$ (**5**) via a metastable tetraferrous sandwich-type precursor.[62] Fractional crystallization is used to separate the two complexes (**4** and **5**) because they differ in charge. The tetra-*n*-butylammonium (TBA) salt of **4** is readily prepared by a metathesis reaction (see Experimental Section).[71] Control of pH is important as POM decomposition is possible at too low (i.e., pH < 2) or too high pH values (i.e., pH > 8).

The ^{31}P NMR spectrum of **4** consists of two peaks corresponding to two symmetry inequivalent distal P atoms. Interestingly, the chemical shift of one peak is similar to

(68) Although only two species (**1** and **2**) were detected in solution and isolated as crystals, it is possible that the mono- and trichlorinated species are present but are not observed by ^{31}P NMR because the chemical shifts (in ppm) of these species overlap the peaks for species **1** and **2**.

(69) Rocchiccioli-Deltcheff, C.; Thouvenot, R. *J. Chem. Res., Synop.* **1977**, *2*, 46−47.

(70) This argument was first used to partially explain why alkaline degradation of β_2-SiW$_{11}$O$_{39}$$^{8-}$ yields γ-SiW$_{10}$O$_{36}$$^{8-}$ rather than β-SiW$_{10}$O$_{37}$$^{10-}$. However, when the (W=O)$^{4+}$ fragment from the rotated M$_3$O$_{13}$ triad adjacent to the lacunary (β_2) site is lost, the intermediate (β-SiW$_{10}$O$_{37}$$^{10-}$) has one tungsten center with three terminal oxygen atoms (in violation of the Lipscomb principle). See: (a) Lipscomb, W. N. *Inorg. Chem.* **1965**, *4*, 132−134. (b) Canny, J.; Tézé, A.; Thouvenot, R.; Hervé, G. *Inorg. Chem.* **1986**, *25*, 2114−2119. (c) Kortz, U.; Jeannin, Y. P.; Tézé, A.; Hervé, G.; Isber, S. *Inorg. Chem.* **1999**, *38*, 3670−3675.
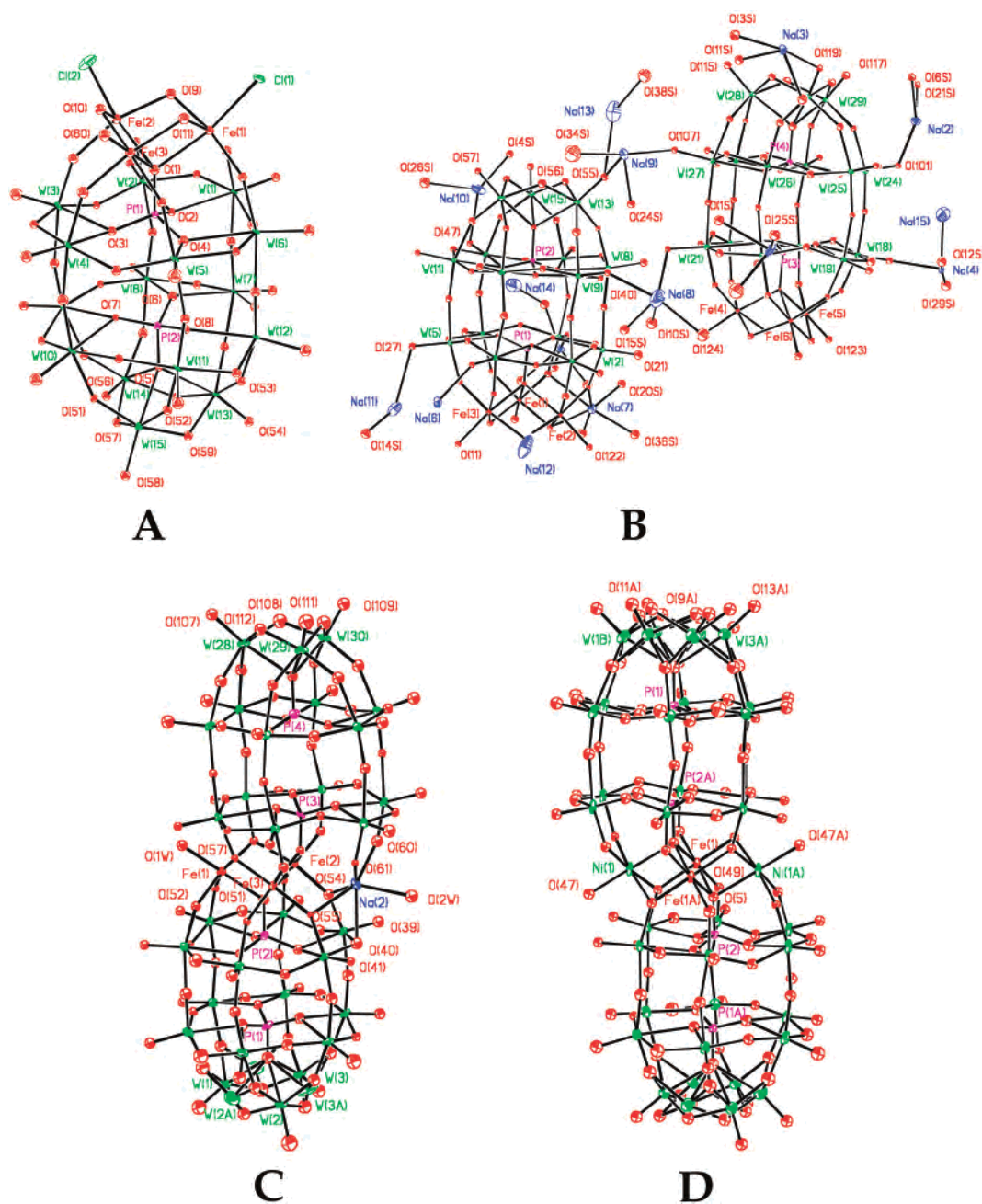
Figure 3. Thermal ellipsoid plots (50% probability surfaces) of the polyanions. (A) Complex **1**. (The Fe1−Cl1, P1−O1, and W13−O54 bond lengths are 2.305(5) Å, 1.573(12) Å, and 1.716(11) Å, respectively. The Fe3−O10−Fe2 and P1−O1−Fe1 angles are 92.2(4)° and 123.6°, respectively.) (B) Complex **2**. (The W13−O56, Fe4−O124, and W2−O21 bond lengths are 1.930(13) Å, 1.998(12) Å, and 1.678 Å, respectively. The W9−O40−W8 and W27−O107−Na9 bond angles are 153.9(6)° and 154.6(6)°, respectively.) (C) Complex **4**. (D) Complex **6**. (Select bond lengths for **4** and **6** are given in Table 3, and a complete list of bond lengths and angles are provided in Supporting Information.)

the tetraferric sandwich, **3**, and the chemical shift of the other peak is similar to the diferric sandwich complex, **5**. This is consistent with a structure having one central β-junction and one central α-junction. The IR spectrum of Na**4** is similar to those previously described for the Cu(II) and Co(II) derivatives of **5** (see structure **7** in Figure 2). All three sandwich-type structures have three metals in the central unit. The split in the ν_3 vibrational mode of the central PO$_4$ units is more pronounced in **4** (1089 and 1053 cm^{-1}) than it is in

the diferric complex, **5** (1089 and 1062 cm^{-1}). This implies there is less structural distortion in the M$_3$ sandwich-type structures compared to the diferric sandwich-complex, **5**.[69]

Reaction of **5** with 2.0 equiv of NiCl$_2$ yields a new mixed-metal sandwich-type POM, $\alpha\beta\beta\alpha$-(Ni^{II}OH$_2$)$_2$Fe$^{III}_2$(P$_2$W$_{15}$-O$_{56}$)$_2^{14-}$ (structure **6** in Figure 2). Unlike the reaction of **5** with Cu(II) or Co(II), two metals are now incorporated into the central unit without subsequent substitution of α_1 tungstens in the α-P$_2$W$_{15}$O$_{56}^{12-}$ units, even when an excess of Ni(II) is present. The ^{31}P NMR spectrum of **6** has one singlet for the symmetry-equivalent P atoms distal to the central Ni$^{II}_2$Fe$^{III}_2$ unit consistent with C_{2h} point group

(71) Katsoulis and Pope have demonstrated that the terminal coordination site on a d-electron-containing metal is dehydrated upon extraction into an organic solvent. See reference 12a.
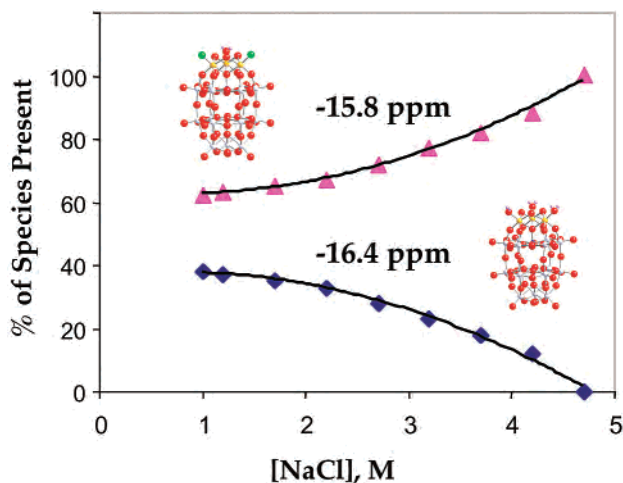
Figure 4. Equilibration of α-$(FeCl)_2(FeOH_2)P_2W_{15}O_{59}{}^{11-}$ (**1**) and α-$(FeOH_2)_3P_2W_{15}O_{59}{}^{9-}$ (**2**). The percentage of each species present (i.e., mole fraction) is plotted as a function of the ionic strength (NaCl concentration) at constant temperature (25 °C) and pH (4).

symmetry for this structure, while the paramagnetism of the $Ni^{II}_2Fe^{III}_2$ unit renders the signal for the proximal P atoms too broad to be observed.[72a] Control of pH ($\sim$2) significantly reduces the number of impurity peaks present in the ^{31}P NMR spectrum. These peaks are attributed to different polar cap rotation isomers.[32,72b] The IR spectrum of Na**6** has W−O stretching bands characteristic of sandwich-type polytungstophosphates. The ν_3 vibrational mode of the central PO_4 unit is split indicating a local symmetry lower than T_d, a feature seen in many sandwich-type POMs.[69] The UV−vis spectrum of **6** is not structurally informative as the intense charge-transfer bands (oxygen-to-tungsten) obscure the Fe- and Ni-centered d−d transitions.

Crystallographic Studies. The X-ray crystal structures of Na**1** and Na**2** reveal single triferric-capped Wells−Dawson structures (Figure 3 and Table 1). In Baker−Figgis notation, both structures are the α (cap rotation) isomer.[72b] The two complexes differ in the types of ligands occupying the terminal coordination sites. Usually, these sites are occupied by water (aqua) ligands if the complex is prepared in aqueous solution. In contrast, two of the three Fe(III)L sites in Na**1** have Cl^- ligands instead. To the best of our knowledge, this is the first example of Cl^- association (at a terminal position) in a POM complex.[73] Na**1** and Na**2** are also the first monomeric Wells−Dawson structures containing complete reconstitution of the M_3 cap by a low-valent metal. An X-ray analysis of a trisubstituted, monomeric Keggin complex has been reported, but it was an A-type trivacant complex, not the B-type trivacant species seen in the defect Wells−Dawson structures.[18] Bond valence sum (BVS) calculations from the X-ray structures of **1** and **2** yield average oxidation states of 3.10 ± 0.06 and 3.08 ± 0.05, respectively, for the Fe atoms.[74] Like many other polyoxometalates, disorder of

Na^+ countercations (in all four structures) makes it impossible to account for the charge balance of the structures by X-ray crystallography alone. As a result, elemental analyses were used instead to precisely determine the total number of Na^+ cations present per formula unit.

The X-ray structure of the triferric POM, Na**4**, (Figure 3C and Table 1) yields a new member of the previously reported M_3 Wells−Dawson sandwich-type POMs. Polyanion **4** is very similar to the previously reported Cu(II)- and Co(II)-substituted diferric sandwich complexes.[57] All three species have one β-junction and one α-junction joining each trivacant POM unit to the central M_3 unit. There are three key differences, however. First, Na**4** does not show simultaneous substitution of two belt (α_1) tungstens with Fe-(III). Second, the outer Fe(III) site in the central M_3 unit does not show significant Jahn−Teller distortion (see Table 3). Third, the fourth position in the central unit of **4** is occupied by a weakly bonded seven-coordinate Na^+ ion (average Na−O bond length 2.45 Å). Finally, bond valence sum calculations from the X-ray structure of **4** yield an average oxidation state of 3.04 ± 0.09 for the Fe atoms.[74]

The X-ray structure of the sodium salt of $\alpha\beta\beta\alpha$-$(Ni^{II}OH_2)_2$-$Fe^{III}_2(P_2W_{15}O_{56})_2$ (Na**6**) reveals that two Ni(II) atoms have replaced the two Na^+ atoms of **5** with simultaneous rearrangement of the structure back to the conventional inter-POM-unit connectivity known as β in Baker−Figgis notation (β-junctions). Each Ni(II) atom is ligated by three oxygen atoms from one of the trivacant α-$P_2W_{15}O_{56}{}^{12-}$ units, two oxygen atoms from the other α-$P_2W_{15}O_{56}{}^{12-}$ unit, and a terminal water ligand (Figure 3D). Bond valence sum calculations from the X-ray structure of Na**6** yield an average oxidation state of 2.25 ± 0.31 for the Ni atoms and 3.16 ± 0.23 for the two Fe atoms.[74] There is rotational disorder in both of the polar W_3O_{13} caps (the two conformations $\alpha\alpha$ and $\beta\beta$ exist in a $\sim$4:1 ratio). Previously, cap disorder in sandwich-type POMs (in the solid state) was observed by Finke and co-workers.[32,75] They attributed additional peaks in the ^{31}P and ^{183}W NMR spectrum of $\alpha\beta\beta\alpha$-$(Zn^{II}OH_2)_2$-$Zn^{II}_2(P_2W_{15}O_{56})_2{}^{16-}$ to the presence of 60° rotations of the polar caps. It is noted in other reports that protonation of bridging oxygen atoms (connecting a cap with the rest of the POM structure) may lead to such cap rotations.[76,77]

Catalysis. TBA**4** and TBA**6** are very good catalysts for the epoxidation of alkenes by H_2O_2 in solution at room temperature. Representative product distributions are given in Table 2. Both complexes are stable (no apparent structural degradation after 75 h in 0.25 M H_2O_2). The selectivity and yields in these reactions approach those of the highly effective Neumann/Khenkin systems (the catalyst used by

(72) (a) Jorris, T. L.; Kozik, M.; Casañ-Pastor, N.; Domaille, P. J.; Finke, R. G.; Miller, W. K.; Baker, L. C. W. *J. Am. Chem. Soc.* **1987**, *109*, 7402−7408. (b) Baker, L. C. W.; Figgis, J. S. *J. Am. Chem. Soc.* **1970**, *92*, 3794−3797.

(73) There is one example of a bridging Cl^- in a POM structure. See: Randall, W. J.; Weakley, T. J. R.; Finke, R. G. *Inorg. Chem.* **1993**, *32*, 1068−1071.

(74) Brown, I. D.; Altermatt, D. *Acta Crystallogr.* **1985**, *B41*, 244−247.

(75) There is also a small amount of cap disorder in one M_3O_{13} unit of Na**4**. Approximately 8% of the POMs have one polar cap rotated by 60° along the long axis of the POM. Although the disorder in Na**4** is not detectable in solution by ^{31}P NMR, the percentage of disorder in the solid state of complex **6** is consistent with the relative ratio observed in solution.

(76) Kawafune, I.; Matsubayashi, G. *Bull. Chem. Soc. Jpn.* **1996**, *69*, 359−365.
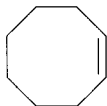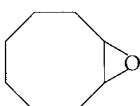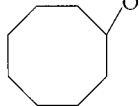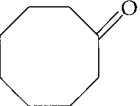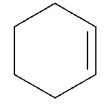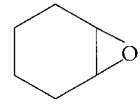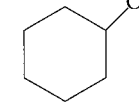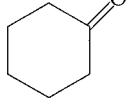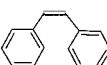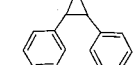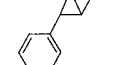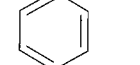
(77) Maksimovskaya, R. I.; Maksimov, G. M. *Zh. Neorg. Khim.* **1995**, *40*, 1363−1368.

Table 2. Product Distributions for Ambient Temperature Oxidation of Alkenes by H_2O_2 Catalyzed by TBA**4** and TBA**6**[a]

Substrate	Products
(Catalyst)	Selectivity (Yields Based on H_2O_2) [Turnovers][b]

(TBA**4**)	99%(94%)[99]	0[c]	1%[1]
(TBA**6**)	99%(99%)[222]	0[c]	0.5%[1]

(TBA**4**)	90%(86%)[9]	0[c]	10%[1]
(TBA**6**)	70%(67%)[7]	0[c]	30%[3]

(TBA**4**)	86%(79%)[50]	14%(11%)[8]	0[c]
(TBA**6**)	96%(71%)[29]	4%(3%)[1.3]	0[c]

[a] Conditions: 25 μL of 30% H_2O_2 (aq) was injected into 1 mL of CH_3CN 4 mM in TBA**4** or TBA**6** and 0.9 M in alkene under Ar to initiate the reaction. Organic products were quantified by GC and GC/MS. [b] Selectivity = (moles of indicated product/moles of all organic products derived from the substrate) × 100; epoxide yields based on peroxide consumed = (moles of epoxide/moles of H_2O_2 consumed) × 100; turnovers = moles of indicated product/moles of catalyst after 30 h reaction time. [c] No products within the detection limit (<0.2%).

Neumann and co-workers is illustrated in Figure 1C.[55,78−82] In addition, yields based on H_2O_2 consumption are high, indicating very little decomposition of H_2O_2 under turnover conditions. The high selectivities for epoxide most likely rule out homolytic mechanisms including Fe-assisted radical-chain breakdown of H_2O_2 and Fenton-type chemistry.

Stability and Formation. The thermal stability of the multi-iron sandwiches (**3**−**5**) were evaluated with careful control of temperature, pH, and ionic strength. At all temperatures (from 20 to 80 °C), pH values (from 3 to 6), and values of ionic strength (NaCl concentrations from 0 to 2.5 M) used, the order of stability (i.e., longevity of the species in solution) was unchanged: **4** ≫ **3** > **5**. The new triferric sandwich (**4**) is significantly more stable than either the diferric (**5**) or tetraferric (**3**) sandwich structures. A

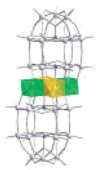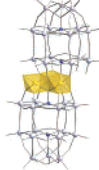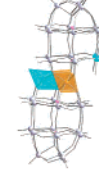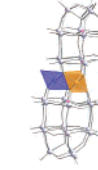(78) Neumann, R.; Gara, M. *J. Am. Chem. Soc.* **1995**, *117*, 5066−5074.
(79) Neumann, R.; Khenkin, A. M. *Inorg. Chem.* **1995**, *34*, 5753−5760.
(80) Neumann, R.; Khenkin, A. M. *J. Mol. Catal. A: Chem.* **1996**, *114*, 169−180.
(81) Neumann, R.; Khenkin, A. M.; Juwiler, D.; Miller, H.; Hara, M. *J. Mol. Catal. A: Chem.* **1997**, *117*, 169−183.
(82) The authors also acknowledge Mizuno and co-workers' recent O_2-based catalytic epoxidation studies as well. See: Nishiyama, Y.; Nakagawa, Y.; Mizuno, N. *Angew. Chem., Int. Ed.* **2001**, *40*, 3639−3641.

Table 3. Average Bond Lengths in Metal Substituted ST-POMs


central unit[a]	Ni_2Fe_2	Fe_3	$CuFe_2$	$CoFe_2$
unit connectivity[b]	αββα	αααα	αααβα	αααβα
$M-O_{ax}$[c]	2.11(2) Å	2.09(4) Å	2.35(1) Å	2.18(4) Å
$M-O_{eq}$[c]	2.08(2) Å	1.97(3) Å	1.97(1) Å	2.01(3) Å
$\Delta M-O$[d]	0.03 Å	0.12 Å	0.38 Å	0.17 Å

[a] Complete formulas (with central units listed first) are $(NiOH_2)_2Fe_2$ $(P_2W_{15}O_{56})_2^{14-}$, $(FeOH_2)Fe_2(P_2W_{15}O_{56})_2^{15-}$, $(CuOH_2)Fe_2(P_2W_{15}O_{56})(P_2Cu_2$-$(OH_2)_4W_{13}O_{52})^{16-}$, and $(CoOH_2)Fe_2(P_2W_{15}O_{56})(P_2Co_2(OH_2)_4W_{13}O_{52})^{16-}$, respectively. [b] Inter-POM-unit connectivities of the sandwich-type POMs (ST-POMs) are for the first cap-belt junction, the first belt-central unit junction, the second belt-central unit junction, and the second belt-cap junction, respectively. [c] Average (axial and equatorial) Ni−O, Fe−O, Cu−O, and Co−O bond lengths, respectively, for the exterior MO_6 octahedra in the central unit. [d] Differences in average axial and equatorial M−O bond lengths.

number of factors may be responsible for these trends. Given the fact that pH, temperature, and ionic strength were all carefully controlled (and the results consistent) over wide ranges, we conclude these factors alone are not directly responsible for this trend in stability. In addition, because the results of the thermal stability experiments suggest that stability is not exclusively a function of the metal population of the central unit, consideration of other structural factors must be made. There are two such factors consistent with the described trend, and we now elaborate each.

One explanation for the different stabilities of sandwich-type structures likely derives from the fact that they are subject to the effects of Baker−Figgis isomerism.[72b] In traditional Keggin and Wells−Dawson structures, 60° cap rotation isomers (denoted as β, γ, δ, and ϵ for one, two, three, or four cap rotations, respectively, in the Keggin complexes) result in structures less thermodynamically stable than the α structure.[72b] Rearrangement of these complexes to the more stable α structure is spontaneous and usually kinetically facile.[83] The relative thermodynamic stabilities of β and α isomers have been measured in situ. Isomerizations of Keggin β-$AlW_{12}O_{40}^{5-}$ and Wells−Dawson β-P_2-$W_{18}O_{62}^{6-}$ to their respective α isomers have $\Delta G°$ values of approximately 2 kcal/mol[59a] and 4 kcal/mol.[59b] As shown in Figure 5A, the junctions between the trivacant Wells−Dawson POM units and the central unit are structurally analogous to the M_3 caps in the parent Wells−Dawson species. Three metal centers from the central unit effectively replace the three "missing" W atoms. Two metal centers are shared by both trivacant POM units (the "internal" metal sites), and each of the two external metal sites of the central unit reconstitutes the remaining vacancy for one trivacant POM unit only. This analysis leads to the reasonable inference that at parity of all other factors (pH, ionic strength,

(83) There are other important factors governing the relative stability of β and α isomers. Previous studies have shown that the nature of the heteroatom plays an important role in determining these relative stabilities. See reference 59a.
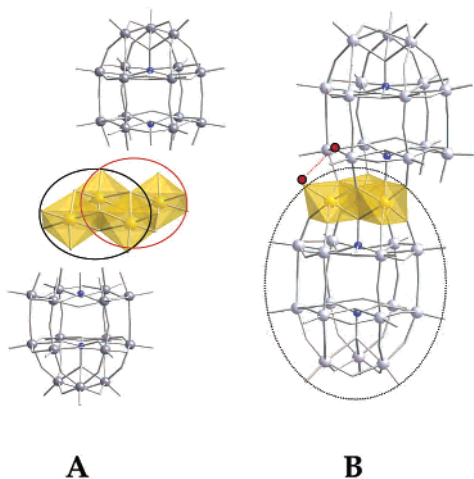
Figure 5. (A) Drawing of a typical sandwich-type polyoxometalate illustrating how the central M_4 unit reconstitutes the M_3 cap of each trivacant Wells–Dawson unit. Two metals of the central M_4 unit are shared by both trivacant POM units. (B) Drawing of $\alpha\alpha\beta\alpha$-(Fe^{III}OH$_2$)Fe$^{III}_2$(P$_2$W$_{15}$O$_{56}$)$_2^{15-}$. The terminal water ligand of the Fe atom in the external position and the bridging oxygen atom of the POM unit are shown in red. A circle is drawn around the POM bound by an α-junction (Baker–Figgis α-isomer) between the trivacant POM unit and the central unit.

countercation, temperature, etc.), a β-junction (i.e. β-isomer) would be less stable than an α-junction (i.e. α-isomer).

A second explanation for the observed stabilities in sandwich-type POMs was first suggested by Finke and co-workers.[32] They proposed that a 60° rotation of each trivacant α-P$_2$W$_{15}$O$_{56}^{12-}$ unit (to generate a structure with two α-junctions from a structure previously having two β-junctions) would bring the terminal ligands of the external metal sites in the central unit significantly closer to the bridging oxygen atoms of the neighboring belt tungsten atoms (Figure 5B).[84] Sandwich structures with two β-junctions or two α-junctions have very similar local coordination polyhedra at the external metal sites of their respective central units. Each metal octahedron at an external site of the central unit has one oxygen atom shared with a P heteroatom, one terminal water ligand, and four oxygen atoms (two from each trivacant POM unit) shared with belt tungsten atoms (α_1 sites). In a structure with two β-junctions, one trivacant POM unit coordinates to the external metal atom via oxygen atoms from two edge-sharing tungsten atoms while the other POM unit coordinates via oxygen atoms from two corner-sharing tungsten atoms (Figure 6A). The same is observed in structures with two α-junctions except that there is a 180° rotation with respect to the β-junctions (Figure 6B). The result of this 180° rotation is the oxo ligands (from each trivacant POM unit) above the axial (xy) plane bisecting each central Fe(III)-octahedron are now below the plane and vice versa. This moves the terminal ligand of the external metal sites in the central unit significantly closer to one of the bridging oxygen atoms of the neighboring belt tungsten atoms (from 2.9 to 2.1 Å).[85]

This suggests that significant repulsion would be present with two pure α-junctions, consistent with Finke's original proposal.[32]

The M_3 sandwich-type POMs have a combination of both α-junctions and β-junctions. Initially, this might suggest that the M_3 sandwich-type structures would not be any more stable than the structures with two α-junctions or two β-junctions, because all three structures would effectively have two such "destabilizing" forces (Baker–Figgis rotation and terminal ligand repulsion). To understand why M_3 sandwiches are unique, consider the ligand coordination geometry at the occupied external metal site of the central unit (Figure 6C). As previously mentioned, sandwich-type structures with two central α-junctions or two central β-junctions have a similar pentadentate coordination geometry at the external metal sites of the central unit, except that one is rotated 180° with respect to the other. The M_3 sandwich, on the other hand, is remarkably different (Figure 5B and 6C). It is bound to two sets of bridging oxygen atoms from each POM unit that are both corner-sharing, unlike structures with two α-junctions or two β-junctions, which involve coordination with one set of corner-sharing and one set of edge-sharing oxygen atoms. The result is a substantially different local coordination geometry for the external MO$_6$ octahedron in the central multimetal unit that allows the metal site to retain its α form (i.e., Baker–Figgis connectivity) while simultaneously allowing the terminal ligand to point away from the bridging oxygen atoms of the POM units (similar to a β junction).

Another interesting feature of the external metal sites in all sandwich-type POMs is their ability to affect the angle (or bend) between each trivacant POM unit (e.g., α-P$_2$-W$_{15}$O$_{56}^{12-}$) and the central unit. This feature came to our attention when we reacted Ni(II) with the diferric lacunary sandwich-type POM, **5**, and got a product which differed not only in the total number of metals incorporated but also in central junction connectivity from that of the Cu(II)- or Co(II)-derivatives ([TM^{II}Fe$^{III}_2$(P$_2$W$_{15}$O$_{56}$)(P$_2$TM$^{II}_2$W$_{13}$O$_{52}$)],$^{16-}$ TM = Cu, Co) prepared in analogous experiments.[57] To understand what factors control such differences in metal incorporation, we first experimentally and independently evaluated the effects of countercation, pH, and temperature, three factors known to impact the formation of POM structures.[22,70b,86–88] The discovery of the role of ionic strength on the reconstitution of the parent Wells–Dawson structures (structures **1** and **2**) reported here prompted us to consider ionic strength as a fourth potential factor. *In all cases, however, no differences in the final structure were*

(84) There is no known crystal structure of a sandwich-type structure with four metals occupying the central unit and two central α junctions. The diferric sandwich structure with two α junctions, complex **5**, has no transition metals occupying the external sites, but rather, it has two weakly bound and very distorted Na-based heptahedra.

(85) The distance between the terminal water ligand of the central unit and the oxo ligand of the belt W atom for an M_4 sandwich-type structure with two α-junctions was determined by using structural data from **3**, rotating each trivacant POM unit by 60°, and then reattaching it to the central unit via *Crystalmaker* (V.5 by David Palmer).

(86) Contant, R.; Ciabrini, J. P. *J. Inorg. Nucl. Chem.* **1981**, *43*, 1525–1528.

(87) Abbessi, M.; Contant, R.; Thouvenot, R.; Hervé, G. *Inorg. Chem.* **1991**, *30*, 1695–1702.

(88) Lyon, D. K.; Miller, W. K.; Novet, T.; Domaille, P. J.; Evitt, E.; Johnson, D. C.; Finke, R. G. *J. Am. Chem. Soc.* **1991**, *113*, 7209–7221.
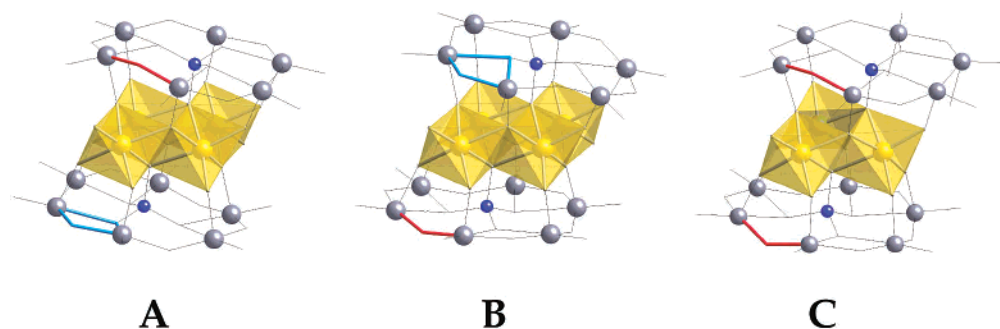
Figure 6. Central units of the multi-iron Wells−Dawson sandwich-type polyoxometalates. (A) Tetraferric sandwich-type structure with two β-junctions. (B) Hypothetical tetraferric sandwich-type structure with two α-junctions. (C) Triferric sandwich-type structure with one α-junction and one β-junction. Only the central multi-iron units and the immediately adjacent "belts" of the trivacant POM units are shown for clarity. Edge-sharing W atoms (at the external site) are shown in blue, and corner-sharing W atoms are shown in red.
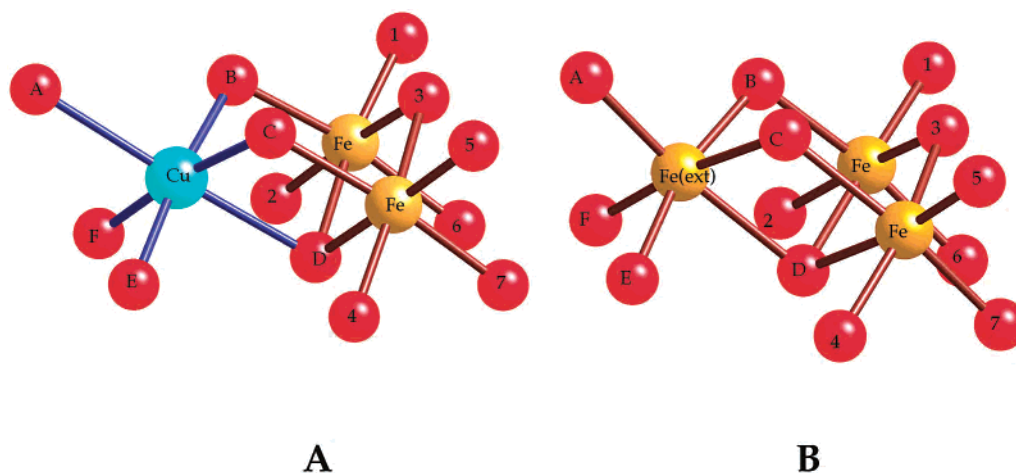
Figure 7. Central units of two representative M_3 sandwich-type polyoxometalates. (A) $Cu^{II}Fe^{III}_2$ central unit (B) $Fe^{III}Fe^{III}_2$ central unit. As the O_1-Fe-O_2 angles in (A) become wider (O_D-Fe-O_B and O_D-Fe-O_C are 83.2(4)° and 83.1(4)°, respectively), the O_3-Fe-O_4 angles in the *xy* plane must become more narrow (O_6-Fe-O_1 and O_7-Fe-O_5 are 90.3(4)° and 91.5(4)°, respectively). Similarly, the O_1-Fe-O_2 angles in (B) are more narrow (O_D-Fe-O_B and O_D-Fe-O_C are 78.4(6)° and 80.0(7)°, respectively); therefore, the O_3-Fe-O_4 angles are wider (O_6-Fe-O_1 and O_7-Fe-O_5 are 94.0(7)° and 94.2(7)°, respectively).

seen as a function of any of these factors.[89] A reasonable explanation for the formation of the different POMs as the d-metal is varied at parity of reaction conditions relates to the Jahn−Teller effect.[90,91]

Table 3 provides bond lengths for the d-metal centers at the external metal sites in four sandwich-type POMs that define the degree of Jahn−Teller distortion in each (differences in the axial and equatorial M−O bonds). The $t_{2g}^6e_g^3$ electron configuration of six-coordinate d^9 Cu(II) results in significant distortion of the local $Cu^{II}(OH_2)O_5$ coordination polyhedron (the difference in axial and equatorial Cu−O bond lengths is 0.38 Å). In contrast, the $t_{2g}^6e_g^2$ configuration of octahedral d^8 Ni(II) shows no such distortion.

Figure 7 shows the central units of the M_3 sandwich-type POMs, $ααβα$-$(Cu^{II}OH_2)Fe^{III}_2(P_2W_{15}O_{56})(P_2Cu^{II}_2(OH_2)_4$-$W_{13}O_{52})^{16-}$ and $ααβα$-$(Fe^{III}OH_2)Fe^{III}_2(P_2W_{15}O_{56})_2^{15-}$. In all of the M_3 sandwich-type structures, one external metal site of the central unit is unoccupied while the metal occupying the other external site is coordinated to both internal Fe(III) atoms (by edge-sharing). Jahn−Teller distortion of the metal atom occupying this site results in a wider angle for the two oxygen atoms between each internal Fe(III) site and the metal occupying the external site (Figure 7A,B). In the case of Cu(II) incorporation, this is due to axial compression and equatorial elongation of the Cu−O bonds (Figure 7A). This means that the O−Fe−O angle in axial plane trans to the O−Fe−O angle adjacent to the Cu(II) site must become narrower. Because both internal Fe(III) sites are coordinated to each trivacant POM unit, the result is the entire structure is bent inward (i.e., closer to 90° with respect to the central unit), thereby narrowing the aperture to the vacant site of the central unit. This effectively closes off the vacant external site and prevents another Cu(II) atom from entering.[92] Consistent with this observation, the X-ray data show that a Na^+ countercation does not coordinate inside the vacant site, as it does in structures **4** and **5**, but stays on the surface of the vacant site instead (Figure 2).

(89) (a) The role of pH was thoroughly evaluated, and careful measurements were taken to control the pH before, during, and after the reactions involving metal incorporation into **5**. Furthermore, in experiments where pH was not controlled, the pH of Ni(II) + **5** (pH = 5.2) lies between that of Co(II) + **5** (pH = 5.6) and Cu(II) + **5** (pH = 3.9). (b) Previous reports have shown that reaction temperature and time can significantly impact the resulting product. See references 32 and 35b.
(90) Deeth, R. J. *Coord. Chem. Rev.* **2001**, *212*, 11−34.
(91) Bersuker, I. B. *Chem. Rev.* **2001**, *101*, 1067−1114.
(92) Furthermore, the X-ray structure of **7** indicates that the two tungsten atoms blocking the aperture of the vacant external metal site are both exchanged for Cu(II) atoms (in the presence of excess Cu(II)).

In contrast, Fe(III) in the triferric sandwich-type complex (**4**) shows significantly less Jahn−Teller distortion (Figure 7B). This results in an aperture to the vacant site that is slightly wider, thus allowing a second equivalent of Fe(III) to be incorporated (as determined by X-ray crystallography). Incorporation of Ni(II) is analogous to Fe(III), because Ni-(II) shows virtually no Jahn−Teller distortion.[93] We were not able to grow diffraction quality crystals of a species with only one Ni(II) present, although ^{31}P NMR and elemental analyses suggest that such a species does exist.

Conclusions. Reactions of trivacant POMs with d-electron-containing transition metals are complex. Typically, only d^0 metals allow full reconstitution of B-type trivacant structures. Complexes **1** and **2**, however, represent the first reconstitution of a trivacant Wells−Dawson structure with a low-valent metal. These complexes are isolated in a synthetic medium of substantial ionic strength (4 M NaCl or greater). While these species are stable in solutions with ionic strength as low as 1 M, lower values (i.e., less than 1 M) always result in rapid (but reversible) decomposition to sandwich-type complexes. Under harsher conditions (high temperature and pH), only the triferric sandwich (**4**) is produced. Thermal stability studies over a range of physical conditions indicate this species is more stable (long-lived) than either the tetraferric (**3**) or diferric (**5**) sandwich-type complexes. The enhanced stability of the triferric species is most likely attributable to the unique coordination environment of its single external metal site. These sites not only play a role in the stability of the sandwich-type complexes, but they also affect how the complex will react with other metals as well. Jahn−Teller distortion of a d-electron metal at an external metal site affects the aperture of the vacant site in the central unit (opposite the site of metal incorporation). The result of a nondistorted Ni(II) reacting with the diferric lacunary complex **5** is the first conventional ($\alpha\beta\beta\alpha$) Wells−Dawson sandwich-type POM with two different metals in its central unit. Metals which show significant Jahn−Teller distortion (Cu(II) and Co(II), for example) incorporate a total of three new metals into the structure (one in the central unit and two in α_1 sites of one trivacant POM unit). Because all previous Wells−Dawson sandwich-type POMs with two central β-junctions contain only one type of metal center ($[(MOH_2)_2M_2(P_2W_{15}O_{56})_2]^{n-}$, where M = Co^{II}, Mn^{II}, Cu^{II}, Ni^{II}, Zn^{II}, and Fe^{III}), the subsequent rearrangement (a possible result of the steric constraints imposed by the terminal water ligands) observed upon Ni(II) incorporation suggests a route to new mixed-metal derivatives.

Supporting Information Available: Complete listing of structure determination parameters, crystal and structure refinement data, atomic coordinates and isotropic displacement coefficients, bond lengths and angles, and anisotropic displacement parameters for Na**1**, Na**2**, Na**4**, and Na**6**. This material is available free of charge via the Internet at http://pubs.acs.org.

IC0112443

(93) The *R*-value of the X-ray structure of the Co$^{II}_3$Fe$^{III}_2$ sandwich was high (R1 ∼ 15%); therefore, the uncertainty in this structure is large enough that it is not specifically discussed in the text with respect to the Jahn−Teller distortion of high-spin octahedral Co(II).